

EXCAVATION AND STUDY OF COMMINGLED HUMAN SKELETAL REMAINS

The Cyprus Institute

Science and Technology in Archaeology and
Culture Research Center (STARC)

Guide No. 2



Authors:

Efthymia Nikita, Anna Karligkioti & Hannah Lee

Reviewers:

Kathryn Marklein, University of Louisville • Ioanna Moutafi, University of Cambridge •
Christina Papageorgopoulou, Democritus University of Thrace • Niki Papakonstantinou,
Aristotle University of Thessaloniki • Paraskevi Tritsaroli, University of Groningen

EXCAVATION AND STUDY OF COMMINGLED HUMAN SKELETAL REMAINS

The Cyprus Institute

Science and Technology in Archaeology and
Culture Research Center (STARC)

Guide No. 2

Authors:

Efthymia Nikita, Anna Karligkioti & Hannah Lee

Reviewers:

Kathryn Marklein, University of Louisville • Ioanna Moutafi, University of Cambridge •
Christina Papageorgopoulou, Democritus University of Thrace • Niki Papakonstantinou,
Aristotle University of Thessaloniki • Paraskevi Tritsaroli, University of Groningen

Version 1.0

Nicosia, 2019

PROMISE



RESEARCH
& INNOVATION
FOUNDATION



The compilation of the manuscript was made possible through generous funding from the European Union Horizon 2020 (Promised, Grant Agreement No 811068) and the Research and Innovation Foundation (People in Motion, EXCELLENCE/1216/0023)

This work is distributed under a creative commons licence (CC BY-NC 2.0).

Nicosia 2019 (Version 1.1, layout edited 2021)

ISBN 978-9963-2858-5-3

CONTENTS

1	Preface
3	Introduction
<hr/>	
5	Excavation
5	Laboratory analysis
6	Bone/tooth inventory
6	Sorting procedures
18	Estimation of the number of individuals
20	Sex assessment
20	Age-at-death estimation
21	Pathological lesions
21	Activity markers
21	Nonmetric traits
21	Morphoscopic traits
21	Metrics
21	Stature estimation
21	Post-mortem bone alteration
<hr/>	
22	Additional Resources
22	References
27	Recording Sheets

PREFACE

This document is the second in a series of guides aimed at promoting best practice in different aspects of archaeological science, produced principally by members of the Science and Technology in Archaeology and Culture Research Center (STARC) of The Cyprus Institute. The current document was largely developed in the context of two projects: *People in Motion* and *Promised*. The implementation of *People in Motion* involved the laboratory study of a large commingled skeletal assemblage from Byzantine Amathus, Cyprus, which came to light in the context of excavations led by the Cypriot Department of Antiquities. Osteological work on this assemblage was co-funded by the European Regional Development Fund and the Republic of Cyprus through the Research and Innovation Foundation (Project: EXCELLENCE/1216/0023). In addition, *Promised* aims at promoting archaeological sciences in the Eastern Mediterranean, with funding from the European Union's Horizon 2020 research and innovation programme under grant agreement No 811068.

Commingled assemblages pose special challenges in their study, nonetheless such a study can reveal key information on the osteobiography of those comprising the assemblage and the funerary practices. In addition, since commingling is both a natural and cultural process, it should be viewed not strictly as an impediment to study (though admittedly methodology has to be adapted and 'traditional' bioarchaeological conclusions are often limited), but as a kind of 'life history' of a skeletal assemblage. In line with the above, the aim of this guide is to cover various aspects of the study of a commingled skeletal assemblage. It should be seen as a supplement to the '*Basic guidelines for the excavation and study of human skeletal remains*; STARC Guide no. 1', which outlines the key general methods for human skeletal excavation and analysis. As the first guide, it focuses on the excavation and study of bioarchaeological assemblages, rather than forensic anthropological material, though many of the practices described are shared between these disciplines. Readers interested in the scientific investigation of multiple burials from forensic contexts are advised to consult the volume by Cox et al. (2008). It cannot be overemphasized that each commingled skeletal assemblage will pose different challenges and any approach to field recovery/excavation and laboratory procedures will have to be adapted to these. Therefore, the current guide is meant to serve only as a general outline, and the described field and lab-based methods should be modified depending on individual circumstances, such as the degree of commingling, sample size, preservation of the material, research questions and other parameters.

A number of excellent edited volumes have been published in the past years, compiling diverse case studies on the retrieval and examination of commingled skeletal remains in archaeological and forensic contexts (Adams and Byrd 2008, 2014; Osterholtz et al. 2014a; Osterholtz 2016). A lot of the information presented here has been drawn from these resources, as well as from other publications and the authors' personal experience. References are given throughout the document but our aim is by no means to provide an exhaustive account of the literature. This document is an open resource and it is anticipated to be updated at regular intervals. We would greatly appreciate any feedback and recommendations for future improvement.

Efthymia Nikita

Anna Karligkioti

Hannah Lee

*For suggestions about how to improve this guide, please contact Efthymia Nikita: e.nikita@cyi.ac.cy

INTRODUCTION

The term “commingling” refers to the intermixing of the remains from more than one individual. This phenomenon is encountered both in archaeological and forensic contexts and poses particular challenges in the retrieval and study of such assemblages. The commingling of elements can occur at different stages during and after the deposition of the bodies and as a result of different factors. The factors that may cause commingling include funerary practices that involve the manipulation of the deceased at various post-mortem stages, intentional interference with the bodies to eliminate incriminating evidence in forensic cases, scavenger activity, underground water and other taphonomic processes (Osterholtz et al. 2014b; Ubelaker 2014). Even without the intervention of any extrinsic factor, commingling will occur as a result of the decomposition processes when multiple individuals are buried together. As the soft tissues disintegrate, skeletal elements will tumble off the pile of bodies, and small elements (e.g. phalanges) will end up at the bottom of the body pile. The way the bodies were deposited, how many individuals were placed in the same grave, the condition of the remains prior to deposition (e.g. fleshed or skeletonised), the amount of free space between the bodies, and other parameters will also affect the degree of commingling (Duday 1985, 2005, 2009; Roksandic 2002).

Commingled assemblages can be classified in different categories. A common division is between small-scale and large-scale commingling. Small-scale commingling is characterised by a small number of disarticulated elements and/or an overall small number of individuals in the assemblage. Note that even in cases of large sample sizes, the degree of commingling

may be classified as small-scale if the skeletal elements are still mostly articulated upon recovery. Large-scale commingling is characterised by large numbers of skeletons with intermixed elements and often very poor preservation (Adams 2014; Byrd and Adams 2003; Mundorff et al. 2014).

An alternative classification is given by Osterholtz et al. (2014b) and is based principally on the duration of use of the multiple burial site:

1. assemblages created through long term usage, and
2. assemblages created through episodic usage.

The main characteristics of each type of assemblage are given in **Table 1** (adaptation of **Figure 1** in Osterholtz et al. 2014b). Osterholtz et al. (2014b: 5) also identify a third type of commingling, that is, lab commingling “that can occur at any stage of analysis or curation”. This type will not be discussed here but the guidelines provided in the following sections to address the other two types of commingling largely apply to cases of lab commingling as well.

The high variability in the characteristics of commingled skeletal assemblages suggests that any strategy for retrieval and study has to be case-specific. The current document aims at covering various approaches, applicable in different types of commingled assemblages, but at the same time it is to be approached as a guide that practitioners will need to adjust to the specific needs of their study. In this direction, it should be read in conjunction with the *‘Basic guidelines for the excavation and study of human skeletal remains; STARC Guide no. 1’*, which outlines the general principles of human skeletal excavation and analysis.

Table 1. Types of commingled assemblages | Adapted from Osterholtz et al. 2014b

	Long term usage	Episodic usage
Formation process	Prolonged tomb use with multiple reopenings to deposit new bodies	A single opening of the tomb to deposit multiple bodies
Characteristics	More pronounced commingling and fragmentation of the remains	Less extensive commingling and better preservation of the remains
Element representation	Variable depending on the nature of the assemblage: <ul style="list-style-type: none"> • Primary long term (bodies decompose at the burial site): representation of smaller elements consistent with the number of individuals • Secondary long term (bodies decomposed elsewhere and then were collected and deposited at the burial site): under-representation of smaller elements 	Generally consistent with the demography of the assemblage
Demography	Reflecting the mortuary program	Reflecting the factor that led to the death and burial of multiple individuals (e.g., plague → mostly very young and very old individuals; warfare → mostly young males)

EXCAVATION

The stratigraphy of mortuary contexts that include the remains of multiple individuals is usually complex, especially in cases where the same location had been used for an extensive period of time. This section provides basic guidelines to the excavation of commingled skeletal remains, which should be adapted on a site by site basis pending the character of each archaeological assemblage and the available resources.

For the steps involved in the excavation of commingled remains, see the guidelines provided in *'Basic guidelines for the excavation and study of human skeletal remains; STARC Guide no. 1'*. What should be stressed here is that grid construction is especially useful when excavating disarticulated commingled remains, where there is a great degree of fragmentation and dispersal of skeletal elements, as it allows for more accurate mapping of individual loose bones and subsequently the examination of patterns in the dispersal of the remains and their association.

As stated in the first volume of this series, stratigraphic excavation is preferred. When excavating commingled remains, it should be remembered that remains found within the same stratigraphic level may be associated, but this is less likely for remains from different stratigraphic deposits. Therefore, when excavating disarticulated remains, one should first look for possible matches within the same deposit (Tuller and Hofmeister 2014). Recognition of partial articulation in the field is necessary as this information may later provide insights to past burial customs.

Burial documentation by means of sketching, photography, and note-taking should follow the guidelines given in STARC Guide no. 1. Total stations or different GPS systems are increasingly used to record burial sites and scattered remains, or even the exact location of individual skeletal elements within the commingled assemblage, since they provide the opportunity to accurately record positional data (see examples in Christensen et al. 2014; Dupras et al. 2012). Therefore, these methods may allow the analysis of the spatial distribution of the remains and reveal patterns of post-depositional processing, as well as assist the reassociation of loose elements based on their relative distance within the assemblage (Naji et al. 2014; Tuller and Hofmeister 2014). An interesting combination of GIS-captured point data on individual skeletal elements and osteobiographic data (age, pathology) was performed by Calleja (2016), who used this approach in visualising the distribution of pathological bones at Bronze Age Tell Abraq.

Considerations when excavating complete skeletons in multiple burials

Attention should be given when digging complete skeletons as it is common that the first elements to be found at a higher elevation than the rest are the skull and the pubic symphysis. These anatomical areas are of great importance in age-at-death and sex estimation, thus care should be taken not to damage them.

LABORATORY ANALYSIS

Each assemblage reaching the lab will have specific properties depending on the depositional environment, the type of commingling (see **Table 1**) and the extent to which articulated elements and elements belonging to the same skeleton more generally have been identified during excavation. **Figure 1** summarises the general procedure that may be followed when studying a commingled assemblage, but this should be adapted according to the nature of

each assemblage under examination. Note that many of these steps are the same as for the general study of human skeletal remains and the reader is advised to consult *'Basic guidelines for the excavation and study of human skeletal remains; STARC Guide no. 1'*. In this section, we will focus exclusively on the methods that are specifically designed for commingled remains.

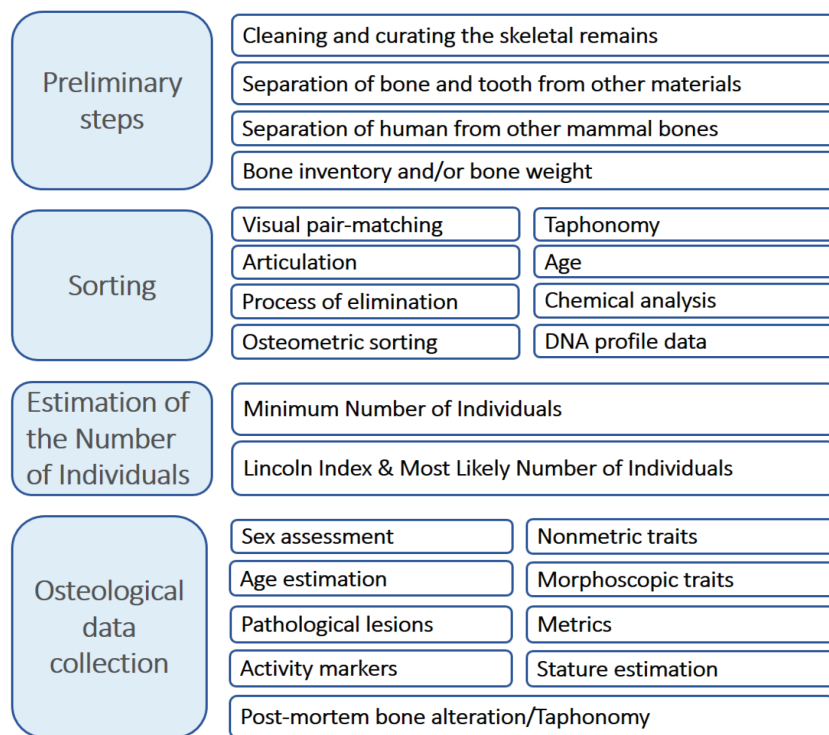


Figure 1. General procedure in the study of commingled assemblages

BONE/TOOTH INVENTORY

The bone and tooth inventory in cases of commingled remains will include each skeletal/dental element or bone/tooth fragment as a separate entry. However, upon sorting the remains, elements belonging to the same individual must be noted as such in the database. As stated in STARC Guide no. 1, bone fragments too small to identify should be divided in broad categories (e.g. cortical bone/trabecular bone, cranial bone/post-cranial bone, axial skeleton/appendicular skeleton), sorted by size class based on maximum dimension, counted and weighted (Outram 2001).

Refitting/conjoining studies can provide important insights to the original position and subsequent relocation and manipulation of the bodies inside the grave (Emberling et al. 2002; Moutafi 2016; Papathanasiou 2009). However, refitting is particularly time consuming, especially in large and highly fragmented assemblages (Knüsel and Robb 2016). When two or more bone fragments are conjoined, they should be input as a single entry in the database with an accompanying note.

SORTING PROCEDURES

During sorting, the bones belonging to each individual are identified (**individuation process**). Depending on the nature of the commingled assemblage (state of bone preservation, sample size, degree of commingling), this step may take place before the inventory and, subsequently, the remains should be inventoried per skeleton rather than per element. The first step of the sorting process involves the **conjoining of fragmentary remains** to the greatest extent possible. Bones should then be sorted by element type, side, and size using the most appropriate among the available techniques: **visual pair-matching, articulation, process of elimination, osteometric comparison, and taphonomy**. Elements that were articulated at the time of recovery should be maintained as a unit. Components of the biological profile (e.g., age-at-death, sex, and stature) may also be useful in the sorting process. Sorting

procedures should be used in conjunction with each other, as well as with contextual scene information (Adams 2014). After all macroscopic techniques have been used, chemical analysis and DNA profile data may be employed.

Visual pair-matching

Visual pair-matching refers to the association of left–right elements based on morphological similarities (Adams and Byrd 2006). Overall bone size and robusticity are the primary factors examined, while nonmetric traits (e.g. third trochanter) or enthesal changes can offer additional help in identifying paired elements. If the elements under study preserve age or sex markers (e.g. unfused epiphyses, pubic symphysis etc.), these are also important to take into consideration in pairing.

Articulation

The size and shape of adjoining bones is correlated as they form a functional joint (Buikstra et al. 1984). However, the strength of association varies depending on the elements considered (Adams and Byrd 2006), thus not all joints will be equally useful in sorting (Puerto et al. 2014 and Figure 2).

HIGH	<ul style="list-style-type: none"> • Cranium – mandible • Vertebrae • 5th lumbar vertebra – sacrum • Humerus – ulna • Innominate – sacrum • Tibia – talus 	<ul style="list-style-type: none"> • Ulna – radius • Metatarsals 2-5 • Metacarpals 2-5 • Tarsals • Tarsals – metatarsals
MODERATE	<ul style="list-style-type: none"> • Cranium – atlas • Tibia – fibula • Femur – tibia • Innominate – femur 	<ul style="list-style-type: none"> • Patella – femur • Navicular (scaphoid) – radius • Carpals* • Carpals – metacarpals
LOW	<ul style="list-style-type: none"> • Metatarsal 1 – other metatarsals • Metacarpal 1 – other metacarpals • Ribs – thoracic vertebrae • Manubrium – clavicle • Humerus – scapula 	

*The articular surface of the pisiform is too small to articulate with confidence

Figure 2. Articulations with associated confidence placed in each fit | Drawn from Table 3 in Adams and Byrd 2006

Reliability of articulations (from Puerto et al. 2014)

- **High reliability ($\geq 90\%$ of correct classification):** vertebrae, sacrum-pelvis.
- **Moderate reliability (60%–90% of correct classification):** temporomandibular joint, atlas–occipital condyles, humerus–ulna, radius–ulna, tibia–fibula, tibia–talus.
- **Low reliability ($\leq 60\%$ of correct classification):** clavicle–scapula, clavicle–manubrium, sternum–ribs, ribs–vertebrae, humerus–scapula, radius–carpals, pelvis–femur, femur–tibia.

Process of elimination

The process of elimination is mostly applicable in cases of small-scale commingling. It is advisable to use this method after articulation and pair-matching have been employed (Adams and Byrd 2006).

Size (osteometric sorting)

Osteometric sorting tests the null hypothesis that the two bones under examination are similar enough in size and shape to have originated from the same individual (Byrd 2008). It may be used for pairing bilateral elements, matching articulated elements, or identifying bones belonging to the same individual based on their relative size (Byrd and LeGarde 2014). Nonetheless, this method is only applicable to well-preserved skeletal elements and it will be of limited, if any, use to highly fragmented material.

Pair-matching

Method 1

Nikita and Lahr (2011) proposed the easiest so far method in pairing bilateral elements based on bone dimensions. The authors provide an Excel macro where different measurements are input and the program considers all possible pairings. If the pairwise differences are below the acceptable user-defined threshold, the right and the left element under examination are given as a potential pair. This method is a way to “prescreen” possible pairs and minimises the time required to visually match the bones. Among the advantages of this method is that it is simple in its implementation, the user can employ any measurement he/she wishes, and additionally to bone measurements, the calculations can incorporate the degree of expression of enthesal changes or osteoarthritis.

Method 2

Most other methods use a reference sample of known paired bones to obtain information on the similarity between homologous measurements. Such methods measure the difference between two potentially paired bones, and then compare this difference to the reference sample to determine whether it is equal to or greater than that expected. In this direction, Byrd and LeGarde (2014) proposed to sum the differences in the values between left and right pair measurements in order to produce the so-called D-value. Subsequently, the D-value is compared to the summed differences of the reference sample for the same measurements. The reference sample serves as a representative source of the left–right differences seen in a population, and in the case of Byrd and LeGarde (2014), it included material from several documented skeletal collections housed in North American institutions. The D-value has zero subtracted, and is then divided by the standard deviation of the reference D-values to produce a t-statistic. Basically, the D-value is being compared against zero to determine whether the difference in size between the elements under examination is significantly different compared to the difference seen in the reference

sample. The t-statistic is then compared to a two-tailed t-distribution to produce a p-value where the degrees of freedom are equal to the reference sample size minus 1. Any p-value that is less than or equal to 0.10 is considered significant, thus the elements are too different in size to have originated from the same individual. A p-value greater than 0.10 does not confirm the elements originated from a single individual, but indicates that the elements may belong to a single individual.

In order to apply the Byrd and LeGarde (2014) method, you need a reference sample from which to estimate the standard deviation of the D-values to produce a t-statistic. If this is not available, you can use the values provided by the authors, so long as you adopt the same measurements as them in your comparisons (**Table 2**). See the original publication for a more detailed description of the measurements.

Table 2. Measurements and reference population data for comparison of paired elements | Adapted from Table 8-9 in Byrd and LeGarde 2014

Skeletal Element	Measurements	N	Standard deviation
Humerus	Maximum length Epicondylar breadth Capitulum-trochlea breadth	113	5.28
	Minimum diameter of diaphysis (in any direction perpendicular to shaft)	73	0.72
Radius	Maximum length Midshaft sagittal diameter Midshaft transverse diameter	100	3.56
	Maximum shaft diameter at the radial tuberosity Maximum shaft diameter distal to the radial tuberosity Minimum shaft diameter distal to the radial tuberosity	52	1.34
	Maximum length Transverse diameter at point of maximum expression of interosseous crest Dorso-volar diameter perpendicular to transverse diameter at the same position along the diaphysis	93	3.60
Ulna	Transverse diameter at point of maximum expression of interosseous crest Dorso-volar diameter perpendicular to transverse diameter at the same position along the diaphysis Minimum diameter of diaphysis along the portion of the bone that includes the interosseous crest	45	1.62

Skeletal Element	Measurements	N	Standard deviation
Femur	Maximum length Epicondylar breadth Maximum head diameter Anterior-posterior subtrochlear diameter Transverse subtrochlear diameter	67	3.99
	Anterior-posterior subtrochlear diameter Transverse subtrochlear diameter	123	1.75
Tibia	Maximum length Maximum breadth of proximal epiphysis Maximum breadth of distal epiphysis	87	3.68
	Maximum diameter at nutrient foramen Transverse diameter at nutrient foramen Minimum anterior-posterior diameter of shaft	44	2.62
Fibula	Maximum length Maximum midshaft diameter	71	2.99

A step-by-step example:

Measurement	Left-side element	Right-side element
Maximum length	492	480
Epicondylar breadth	85	77
Maximum head diameter	50	51
Anterior-posterior subtrochlear diameter	25	28
Transverse subtrochlear diameter	26	31
D	2.757	
Reference sample standard deviation (from Table 2)	3.99	
t (calculated as $ D-0 /3.99$)	0.691	
p (from t-distribution, d.f. = 66, 2 tails)	0.492*	

*You can easily calculate this value in Excel using the command =TDIST(t, d.f.,2), whereby t is the t value you have already estimated (in our case 0.691) and d.f., the degrees of freedom, are equal to the sample size minus 1 (in our case 67-1 = 66). In our example, we have =TDIST(0.691,66,2) = 0.492

Vickers et al. (2015) conducted a validation study of the method proposed in Byrd and LeGarde (2014). Although they found that the number of potential pairs requiring visual matching was considerably reduced, they highlighted three serious shortcomings of this method: (i) violation of the normality assumption for use of a t-score approach, (ii) lack of accountancy of bilateral asymmetry, and (iii) high rate of false rejections.

Lynch et al. (2018) more recently proposed two variants of this model and found the two new models (Models B and C in Table 3) to outperform the original one (Model A in Table 3). Table 3 presents the calculations involved in each model.

Method 3

An alternative method for osteometric pair-matching was proposed by Thomas et al. (2013). This method compares a calculated M-statistic, which expresses the metric similarity of bilateral elements, to a reference sample. The M-statistic is calculated using the following equation, where L and R represent left and right bilateral measurements, respectively:

$$M = \frac{|L - R|}{\left(\frac{L + R}{2}\right)}$$

Pairs of skeletal elements are considered likely homologs if the M-statistic approaches zero, and this is statistically evaluated by means of confidence intervals calculated from reference samples. The reference samples come from several skeletal collections and databases, largely the same as the material used in the Byrd and LeGarde (2014) method.

The null hypothesis that two homologs are from the same individual can be tested by calculating the value of M for each measurement for the bones in question and comparing it to the 90th and 95th percentiles or the maximum value

Table 3. Different models for osteometric pairing (from Figure 1 in Lynch et al. 2018)

Model A	Model B	Model C
$D = \sum a_i - b_i$	$D = \sum a_i - b_i$	$D = \sum a_i - b_i $
$\bar{x} = 0$	$\bar{x} = \frac{\sum D_{ref}}{N}$	$\bar{x} = \frac{\sum D_{ref}}{N}$
$t = \frac{D_{com} - \bar{x}}{S_{D_{ref}}}$	$t = \frac{D_{com} - \bar{x}}{S_{D_{ref}}}$	$t = \frac{D_{com} - \bar{x}}{S_{D_{ref}}}$

Key: a and b indicate the left and right-side measurements, respectively; i is the index of the number of measurements; N is the reference sample size; ref and com refer to the reference and comparison samples, respectively

of M from the reference database (given in **Table 4**). If the value of M is greater than that for the chosen percentile, the null hypothesis can be rejected, suggesting that the bones under examination are unlikely to have originated from the same individual. Rather than using the sum of multiple measurements as seen in the statistical models of Byrd and LeGarde (2014), this method examines each measure independently. Therefore, it is useful for evaluating highly fragmented commingled assemblages; however, it is also considered statistically weak.

Table 4. Maximum values and the 90th and 95th percentiles for the M statistic (drawn from Table 2 in Thomas et al. 2013)

Skeletal Element	Measurement*	N	90th	95th	Max M
Clavicle	Max Length	104	0.049	0.056	0.081
	A-P Diameter Midshaft	93	0.182	0.154	0.222
	M-L Diameter Midshaft	92	0.180	0.200	0.353
Scapula	Height	102	0.031	0.039	0.077
	Breadth	115	0.032	0.040	0.064
	Max Height Glenoid Fossa	67	0.050	0.061	0.092
	Max Breadth Glenoid Fossa	68	0.054	0.058	0.082
Humerus	Max Length	152	0.021	0.026	0.071
	Epicondylar Breadth	135	0.034	0.047	0.079
	Capitulum-Trochlea Breadth	57	0.039	0.052	0.067
	Head Diameter	128	0.040	0.043	0.089
	A-P Head Breadth	46	0.034	0.038	0.043
	Max Diameter Midshaft	118	0.091	0.099	0.160
	Min Diameter Midshaft	138	0.074	0.101	0.162
Min Diameter Diaphysis	75	0.066	0.079	0.101	

Skeletal Element	Measurement*	N	90th	95th	Max M
Radius	Length	134	0.019	0.029	0.064
	A-P Diameter Midshaft	104	0.089	0.098	0.154
	M-L Diameter Midshaft	104	0.097	0.117	0.143
	Max Diameter at Radial Tuberosity	57	0.057	0.079	0.096
	Max Diameter of Diaphysis Distal to Radial Tuberosity	56	0.075	0.106	0.167
	Min Diameter of Diaphysis Distal to Radial Tuberosity	72	0.068	0.073	0.091
Ulna	Length	129	0.022	0.026	0.041
	Dorso-Volar Diameter	116	0.129	0.186	0.533
	Transverse Diameter	132	0.116	0.160	0.375
	Physiological Length	85	0.022	0.027	0.039
	Min Diameter Osseous Crest	48	0.071	0.087	0.102
	Min Diameter	50	0.062	0.081	0.095
Os Coxa	Height	133	0.019	0.023	0.051
	Iliac Breadth	132	0.025	0.030	0.077
	Max Thickness at Sciatic Notch	68	0.092	0.118	0.158
	Max Diameter of Acetabulum	46	0.031	0.035	0.046
Femur	Max Length	109	0.014	0.015	0.020
	Epicondylar Length	99	0.014	0.015	0.021
	Epicondylar Breadth	108	0.022	0.025	0.063
	Head Diameter	122	0.026	0.037	0.048
	A-P Subtrochlear Diameter	140	0.071	0.095	0.129
	Transverse Subtrochlear Diameter	126	0.066	0.094	0.163
	A-P Diameter Midshaft	79	0.053	0.067	0.083
	S-I Neck Diameter	53	0.056	0.063	0.082
Tibia	Length	136	0.014	0.015	0.033
	Max Breadth of the Prox Epiphysis	104	0.026	0.031	0.041
	Max Breadth of the Dist Epiphysis	101	0.042	0.051	0.078
	Max Diameter at Nutrient Foramen	138	0.073	0.095	0.127
	Transverse Diameter at Nutrient Foramen	122	0.083	0.097	0.424
	Max A-P Diameter Distal to Popliteal Line	47	0.060	0.073	0.090
	Min A-P Diameter Distal to Popliteal Line	49	0.074	0.086	0.094

Skeletal Element	Measurement*	N	90th	95th	Max M
Fibula	Length	107	0.013	0.016	0.041
	Max Diameter Midshaft	75	0.092	0.118	0.133
	Min Diameter of Diaphysis	58	0.108	0.128	0.149
Calcaneus	Length	73	0.029	0.033	0.056
	Middle Breadth	66	0.045	0.050	0.085

*For a definition of the measurements, see Thomas et al. (2013)

Key: Max = maximum; Min = minimum

Articulating Bone Portions

Models for comparing adjoining bones are based on the difference in size of the articulating surfaces of these bones (Buikstra et al. 1984). For example, to test if an os coxa and a femur belong to the same individual, we subtract the maximum femoral head diameter from the maximum acetabulum diameter. The model takes the general form (Byrd and LeGarde 2014):

$$D = c_i - d_j$$

where measurement i of bone c is subtracted from measurement j of bone d. The D value obtained from the skeletons under study is compared against the mean D value calculated from reference data in order to test the null hypothesis that the size difference between the two

adjoining bones is small enough for them to come from the same individual. Byrd and LeGarde (2014) have used a broad American sample as reference. In order to obtain a p-value, the difference of D from the reference data mean is divided by the reference data standard deviation and evaluated against the two-tailed t-distribution.

As was the case for pairing skeletal elements, to apply the Byrd and LeGarde (2014) method, a reference sample is necessary to estimate the standard deviation and the mean value of the D-values in order to produce a t-statistic. If this is not available, the values provided by the authors may be used, so long as the same measurements as theirs are adopted in the comparisons (Table 5). See the original publication for a more detailed description of the measurements.

Table 5. Joints and reference population data for comparison of articulating elements (from Table 8-10 in Byrd and LeGarde 2014)

Joint	D	N	Mean	Stand dev
Shoulder	Humerus head A-P breath – Glenoid fossa max breath	159	6.61	2.35
Elbow A	Humerus capitulum-trochlea breadth – Radius head max diam	156	20.99	2.38
Elbow B	Humerus capitulum-trochlea breadth – Breadth at distal end of ulnar semi-lunar notch	166	20.49	2.39
Hip	Max diam of acetabulum – Femur max head diam	176	9.66	1.67
Knee	Femur epicondylar breadth – Tibia max breadth of proximal epiphysis	270	5.20	2.20
Ankle	Tibia max breadth of distal epiphysis –Talus min breadth of articular surface	147	17.91	2.85

A step-by-step example:

Measurement	Value
Femur epicondylar breadth	88
Tibia max breadth of proximal epiphysis	86.7
D	1.3
Reference sample mean (N = 270)	5.2
Reference sample standard deviation (N = 270)	2.2
t (calculated as $ D-5.2 /2.2$)	1.77
p (for t-distribution with d.f.= 269, 2 tails)	0.0779

Other authors have developed regression equations for matching articulating elements (for example, see Anastopoulou et al. 2018 and 2019 for regression equations for matching articulating os coxae, femora, tibiae, tali and calcanei).

Other Bone Portions

Byrd and Adams (2003) propose the following approach for comparing the size of different bones: The measurements obtained on a bone are summed and the natural logarithm of this sum is used in regression models. To derive the t-value from the case specimens, the following model should be used (Byrd and LeGarde 2014):

$$t = |\hat{y} - y_i| / \left[(S.E.) \sqrt{\left[1 + \left(\frac{1}{N}\right) + \frac{(x_i - \hat{x})^2}{NS_x^2} \right]} \right]$$

where \hat{y} is the predicted value from the regression model, y_i the dependent variable value of the case specimen, S.E. is the regression model standard error, N is the sample size used in the calculation of the regression model, x_i is the independent variable value of the case specimen, \hat{x} is the reference sample mean for the independent variable,

and S_x is the reference sample standard deviation of the independent variable. At large sample sizes ($N > 200$), a simpler model can be derived by using the difference between the case specimen dependent variable value and the predicted value divided by the standard error of the estimate:

$$t = \frac{|\hat{y} - y_i|}{S.E.}$$

The value resulting from this calculation is then compared to the t distribution. For step-by-step examples and selected reference data, see Byrd and LeGarde (2014).

Taphonomy

Taphonomic patterns (see section 'Post-mortem bone alteration' in 'Basic guidelines for the excavation and study of human skeletal remains; STARC Guide no. 1') can be used for skeletal reassociation. Skeletal remains in different locations within a grave may be exposed to different taphonomic agents and the resulting bone alterations may be used to sort individuals exposed to different taphonomic processes during primary inhumation, who became commingled at a later stage. However, taphonomy must be used with caution in the sorting process as taphonomic differences can also be observed on the remains of a single individual, especially if they occurred post-disarticulation.

Age

The size and maturity of the skeletal remains can be particularly helpful in discriminating the remains of adult from nonadult remains. In this direction, a method has been proposed by Schaefer (2014) in order to identify commingling among juvenile remains or between juvenile and adult remains based on the stage of epiphyseal union (Figures 3-5).

Figures 3-4: The tree diagrams in Figures 3 and 4 demonstrate the general sequence in epiphyseal union (adapted from Schaefer 2014). In each figure the central "tree trunk" represents the modal sequence pattern, while variations to this pattern are shown as "tree branches." To the left of the trunk are epiphyses that occasionally commence/complete union before the "trunk".

Figures 5: To the left of the antenna diagram are the epiphyses that have completed union before the reference epiphysis, which is given in the middle of the diagram. The ratios in the right-hand boxes express the number of individuals with fused named epiphysis, while the reference epiphysis was still open to the number of individuals where both epiphyses were in the process of uniting.

“Beginning” union

Begins union prior to reference epiphysis in a minority of cases

Modal sequence pattern

Begins union subsequent to reference epiphysis in a minority of cases

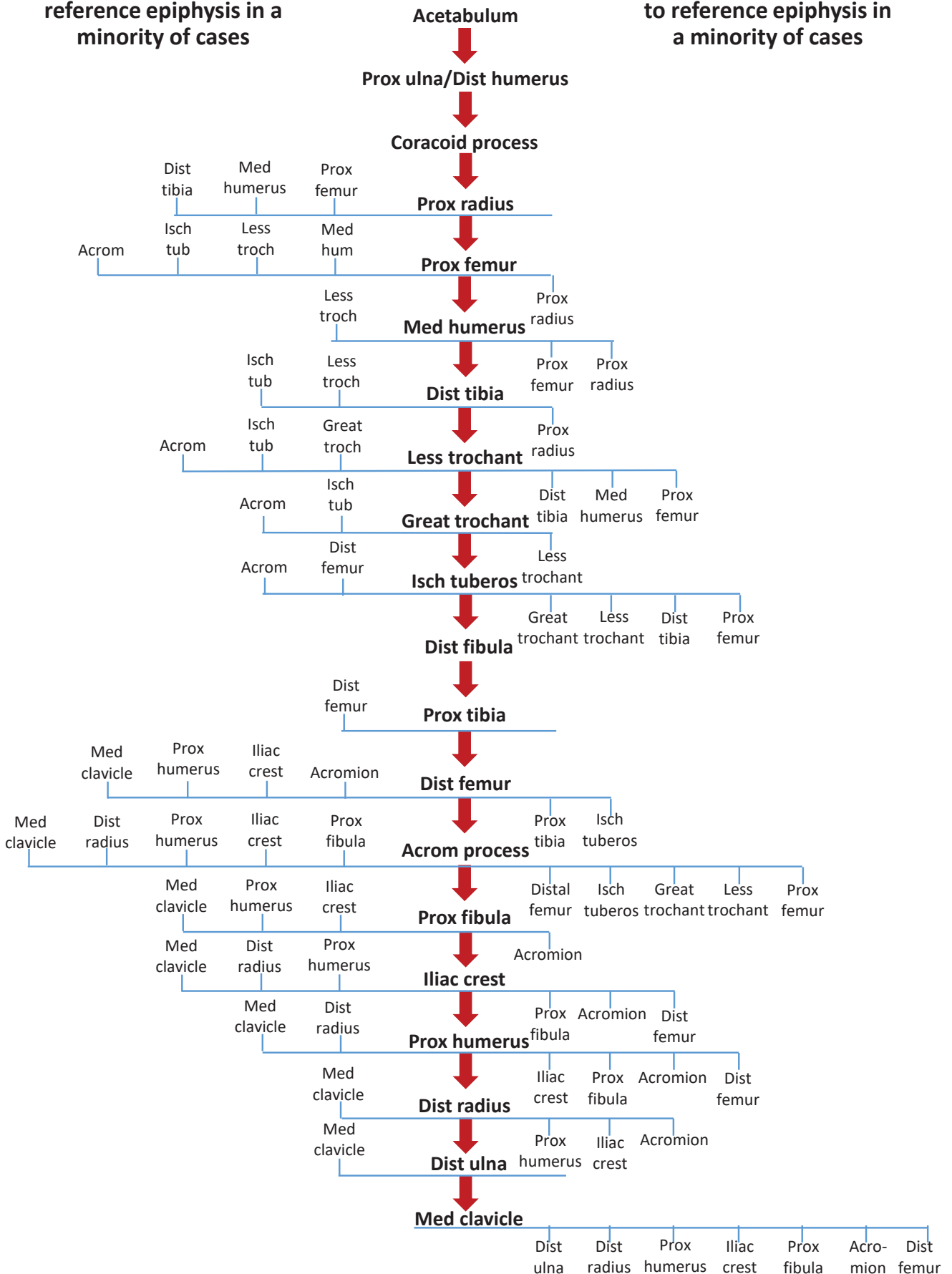


Figure 3. Tree diagram demonstrating the overall sequence in which epiphyses begin union (redrawn from Schaefer 2014)

“Complete” union

Completes union prior to reference epiphysis in a minority of cases

Modal sequence pattern

Completes union subsequent to reference epiphysis in a minority of cases

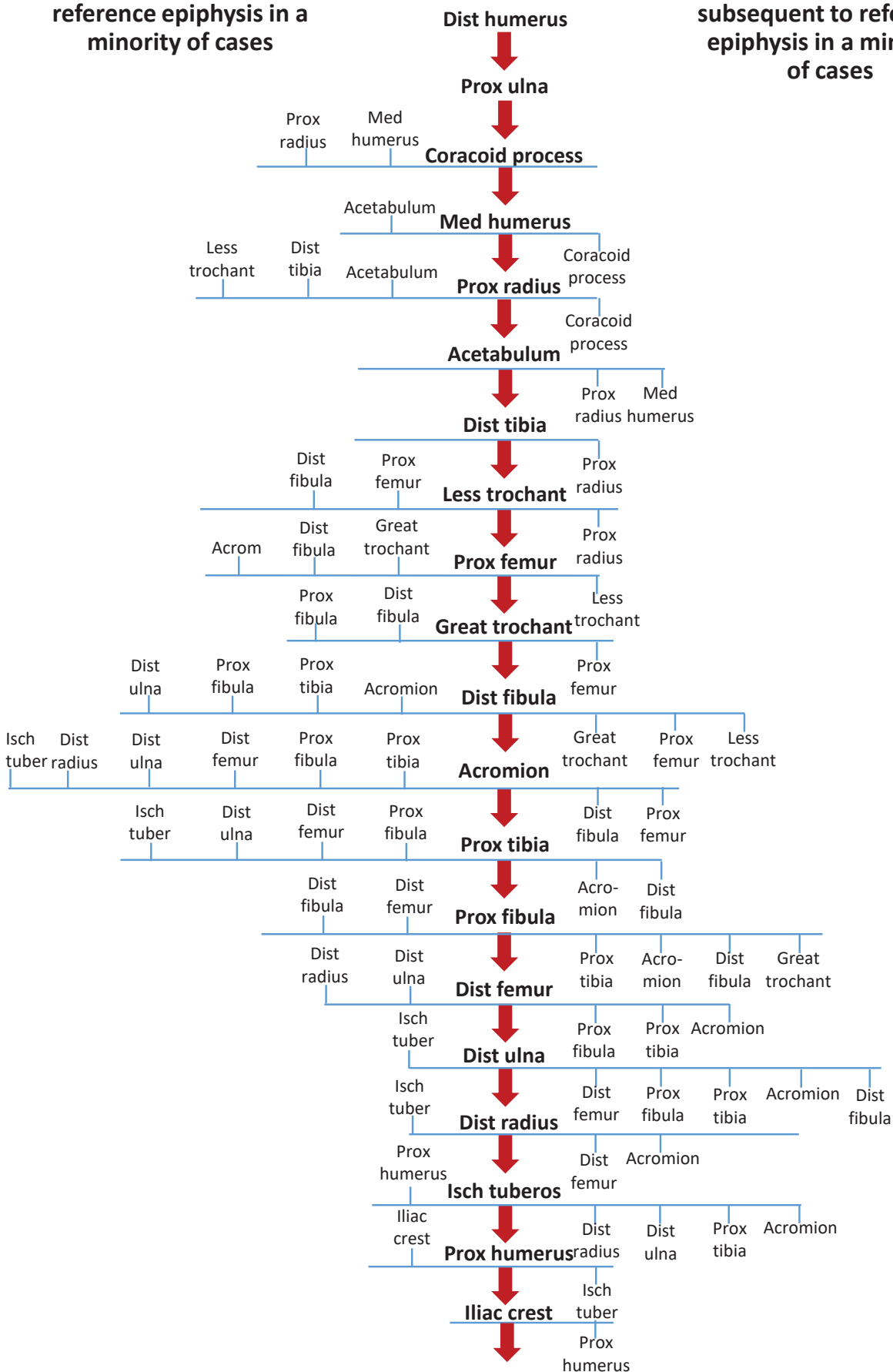


Figure 4. Tree diagram demonstrating the overall sequence in which epiphyses complete union (redrawn from Schaefer 2014)

always completes before
reference epiphysis begins

sometimes completes before
reference epiphysis begins

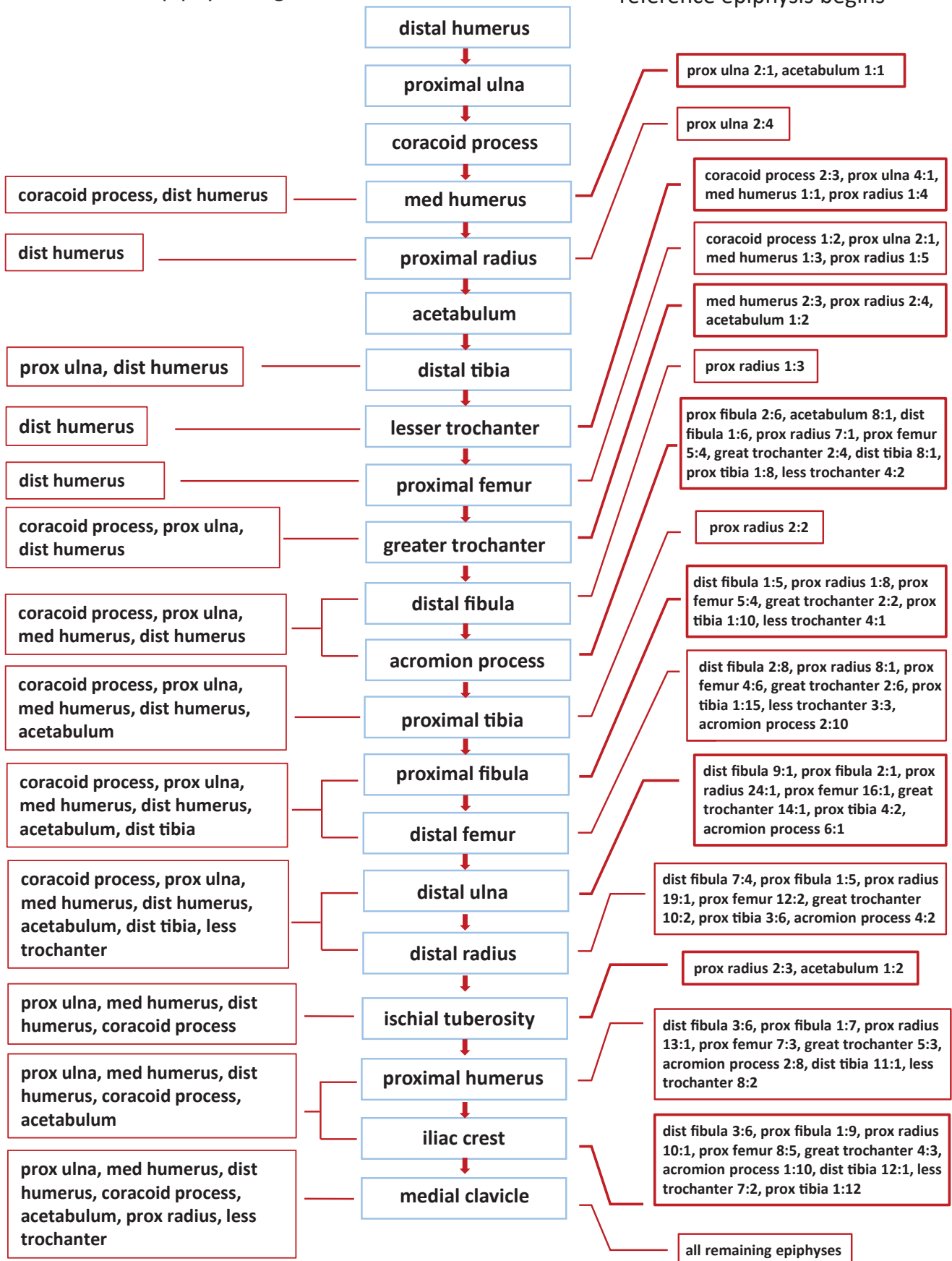


Figure 5. Antenna diagram (redrawn from Schaefer 2014)

Chemical analysis

Recent research using X-ray fluorescence (XRF) spectrometry and laser ablation inductively coupled plasma mass spectrometry (LA-ICP-MS) have shown promise in determining whether a set of remains belongs to a single or multiple individuals by analysing the elemental concentration in human bones (Castro et al. 2010; Gonzales-Rodriguez and Fowler 2013; Perrone et al. 2014; Stevens 2016). Note that the former technique is non-destructive, while the latter requires part of the bone to be destroyed during analysis. Inter-skeletal differences in bone mineral composition may be due to in vivo uptake from food and water, metabolic functions, chemical exposure or other means of absorption (Perrone et al. 2014). A confounding factor is that trace elements are stored differently throughout the human skeleton (Pemmer et al. 2013; Price 1989; Wittmers et al. 1988), thus, intra-individual variability in elemental composition may exceed inter-individual variability (Budd et al. 2000; Finnegan 1988; Grupe 1988). Trace elemental signatures also vary throughout an individual's lifespan due to age-related metabolic and physiological functions (Darrah et al. 2009). Another confounding factor is post-mortem contamination (diagenesis), which may alter the elemental concentrations in buried human bones. However, surface contamination should not be an issue as x-rays penetrate the bone surface by several millimetres during chemical analysis (Shackley 2011).

DNA profile data

DNA analysis is increasingly employed in commingling cases (e.g. Holland et al. 2003; Just et al. 2009; Mundorff et al. 2014; Parsons et al. 2007; Primorac 2004; Verdugo et al. 2017). In osteoarchaeological analysis, ancient DNA data mostly aim at addressing issues of kinship, migration patterns and genetic diseases, while in forensic contexts the aim of DNA analysis is the identification of the unknown individuals. Given its cost and destructive nature, DNA analysis should be best used in conjunction with the context of the remains and the results of the macroscopic skeletal analysis (Puerto et al. 2014).

Hines et al. (2014) present a practical protocol for the effective sampling for partial/commingled remains, depending on the body parts that may be encountered in any given case. Assessment of the success rates for the various elements allowed categorization of sample success rates into four tiers (Table 6).

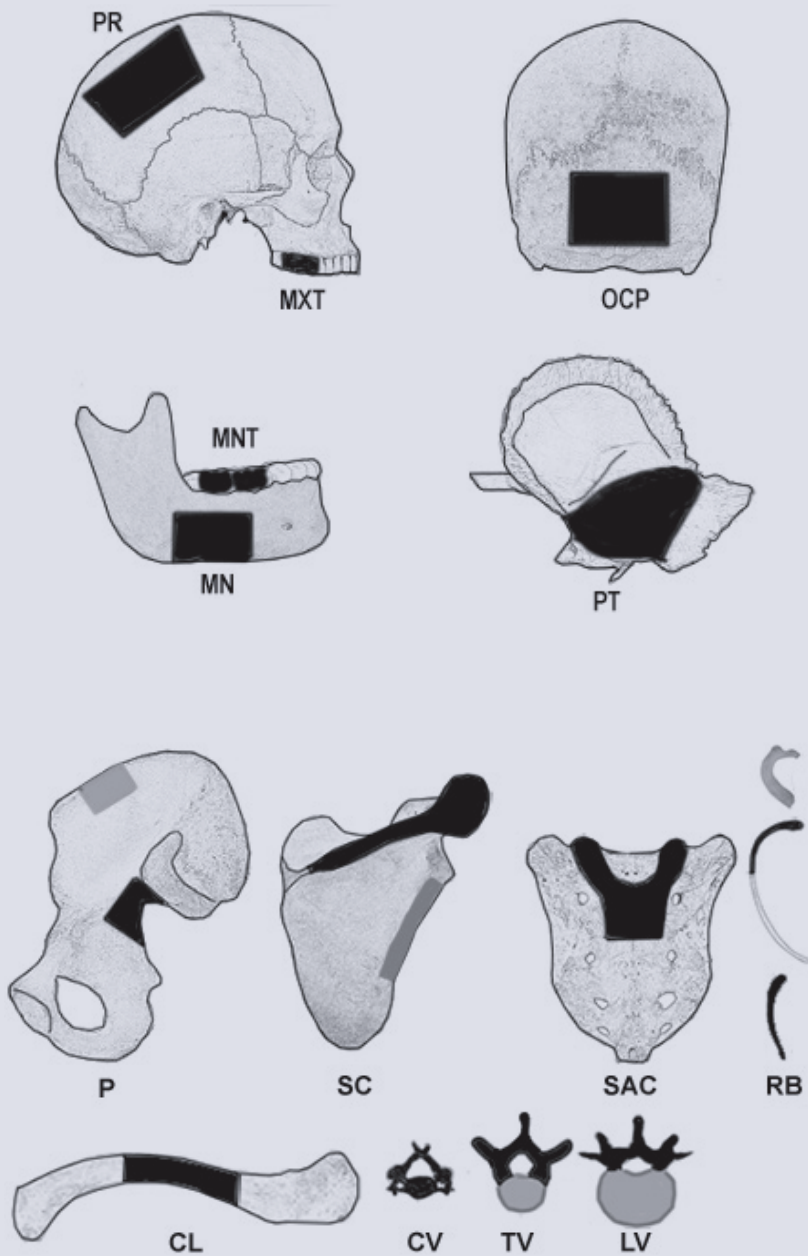
Table 7 summarises the procedure Hines et al. (2014) recommend for sampling skeletal remains for DNA analysis. Figure 7 shows the locations for sampling per element. In black you see the first priority areas and in grey the second priority areas. Note that teeth should be extracted whole. Anterior maxillary or mandibular molars or premolars are preferred. The teeth sampled should not have caries or post-mortem damage, if possible.

Table 6. Skeletal elements per tier based on success rates in extracting DNA (drawn from Hines et al. 2014)

Tier 1 High success rates	Tier 2 Moderate success rates	Tier 3 Successful less than half the time	Tier 4 Even less successful
Teeth	Os coxa	Ribs	Clavicle
Talus & other tarsals	Fibula	Cranium	Ulna
Petrous portion of temporal	Scapula	Humerus	Radius
Femur	Mandibular body		
Vertebrae	Metacarpals		
Tibia			
Metatarsals			

Table 7. Procedure for sampling skeletal remains for DNA analysis per Hines et al. (2014)

BEFORE SAMPLING	
1.	Take photo of the element in its original condition (include photo scale and label)
2.	Clean tools: 1. Water rinse to remove adherent material • 2. Rinse with a solution of 10% commercial bleach or wipe with bleach • 3. Rinse with ethanol
DURING SAMPLING	
1.	Use protective equipment (gloves, mask, safety glasses) to avoid contamination
2.	Aim for sampling 12 to 25 grams (4 grams is minimal but acceptable)
3.	Avoid sampling areas where the bone is discolored
4.	Use particulate/fume extraction facilities if multiple samples are being taken, particularly in enclosed spaces
5.	Place each sample in its own container, with a unique specimen number. It is important that the specimen is completely dried before packaging, and breathable (eg. paper) packaging, should be used where practical
AFTER SAMPLING	
1.	Take photo of the sampled element with the extracted location clearly shown, the extracted sample code, and a photo scale
2.	Do not expose the sample to conditions of elevated heat or humidity



For an alternative approach in collecting femur, rib, and tooth samples for DNA analysis in forensic settings, see Westen et al. (2008).

ESTIMATION OF THE NUMBER OF INDIVIDUALS

Estimates of the number of individuals present in a commingled assemblage fall under two broad categories: Minimum Number of Individuals (MNI) estimators and Most Likely Number of Individuals (MLNI) estimators.

Minimum Number of Individuals (MNI)

The MNI expresses the least number of individuals required to account for the skeletal elements present in the assemblage that has been recovered. The most common way to estimate the MNI is by sorting the bones by side and element and then taking the most frequent element as the estimate. In other words, the MNI is equal to the most repeated element after sorting by element and side: Max (L, R) (White 1953). In cases of fragmentary remains, make sure that there is an overlap of anatomical features on the fragmented remains (e.g. greater trochanter) in order to avoid counting the same individuals more than once.

A variant of the MNI is the Grand Minimum Total (GMT) and is calculated as $L + R - P$, where P signifies the number of bone pairs (Chaplin 1971). This technique assumes that unpaired bones originate from different individuals (Adams and Konigsberg 2004). It requires the accurate identification of all pairs between the bilateral elements of the assemblage, while incorrect matches will bias the results.

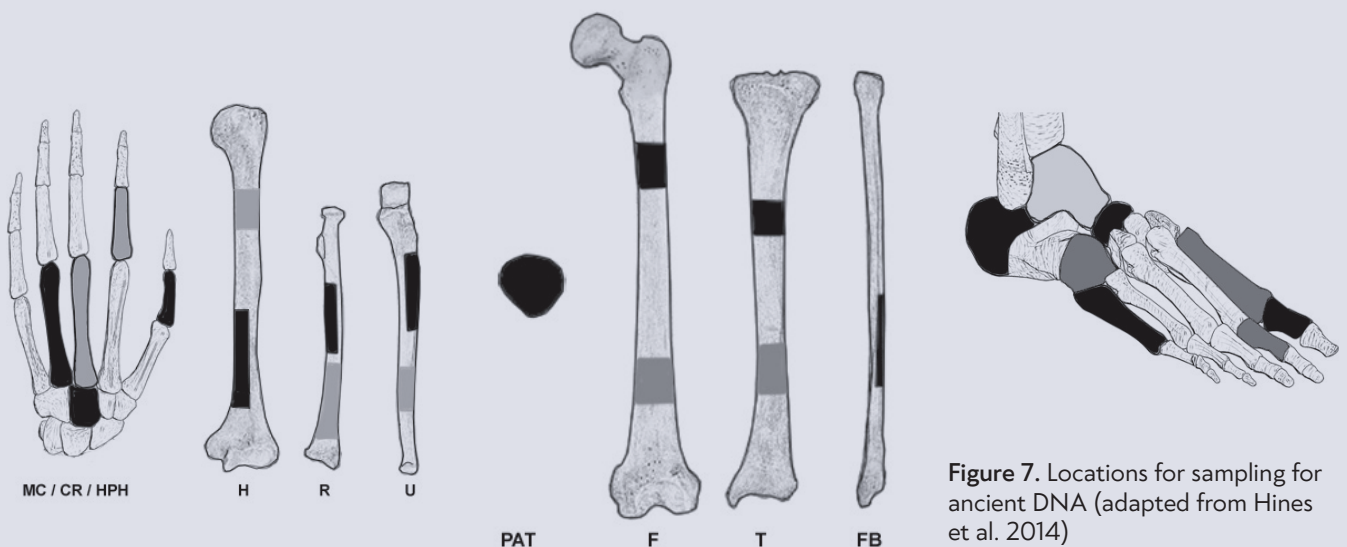


Figure 7. Locations for sampling for ancient DNA (adapted from Hines et al. 2014)

Example

Assume that we have an assemblage where femora are the most numerous elements recovered. We have 145 left, 130 right, and 95 pairs of femora in our sample. Then:

$$MNI = \text{Max}(L, R) = 145$$

$$GMT = L + R - P = 180$$

In some contexts, MNI may be inferred from the biological profile of the elements. For example, the presence of some elements clearly suggestive of a male individual and others suggestive of a female, indicate that at least two individuals were buried together. Similarly, the observation of considerable differences in bone size, especially between bilateral or adjoining elements, also supports the presence of multiple individuals.

Even though MNI and GMT can provide useful information on the smallest number of individuals that comprise the assemblage, they underestimate the true sample size whenever the recovery rates are less than 100%, which is often the case in archaeological assemblages (Konigsberg and Adams 2014; Nikita and Lahr 2011).

Lincoln Index (LI) and the Most Likely Number of Individuals (MLNI)

LI and MLNI estimators assess the initial number of individuals that comprised the assemblage under study based on the fact that the probability of identifying P pairs between R right and L left bones from N initial individuals follows the hypergeometric distribution (Adams and Konigsberg 2004). When using the LI or MLNI, it is important that probabilities of sampling the left and right sides within individuals are independent. An estimate of the original assemblage represented by the skeletal elements is determined by:

$$LI = \frac{L \times R}{P}$$

The LI is a good approximation of the MLNI. A modification to this formula to account for sample bias was proposed by Seber (1973). Adams and Konigsberg (2004) have shown that Seber's formula represents the maximum likelihood estimate and refer to it as the Most Likely Number of Individuals (MLNI). It is calculated as:

$$MLNI = \left\lfloor \frac{(L + 1)(R + 1)}{P + 1} - 1 \right\rfloor$$

where the symbols $\lfloor \cdot \rfloor$ represent the floor function that removes any decimal points.

With the MLNI, it is possible to calculate confidence intervals. An approximate confidence interval can be calculated using the following equation:

$$v^* = \frac{(L + 1)(R + 1)(L - P)(R - P)}{(P + 1)^2(P + 2)}$$

For example, an approximate 95% CI can be calculated as $MLNI \pm 1.96\sqrt{v^*}$. However, because the number of individuals, N , follows a discrete distribution, it is not statistically accurate to give customary confidence intervals, such as 95% intervals. Adams and Konigsberg (2004) propose using instead the highest density region (HDR). For more information on the HDR and its calculation, see Adams and Konigsberg (2004) and the website <http://konig.la.utk.edu/MLNI.html>.

As with GMT, this method relies on the ability to make accurate pair matches between elements. Therefore, it is important for the elements to be well-preserved (Konigsberg and Adams 2014).

The accuracy of MLNI estimators is expected to improve when multiple skeletal elements are taken into account simultaneously instead of using only the most abundant bone. For this reason, the following equations have been proposed (Nikita 2014):

$$N = \frac{R_1L_1 + R_2L_2 + \dots + R_nL_n}{P}$$

$$N = \frac{(R_1 + R_2 + \dots + R_n + L_1 + L_2 + \dots + L_n)^2}{4nP}$$

$$N = \frac{(R_1 + L_1)^2 + (R_2 + L_2)^2 + \dots + (R_n + L_n)^2}{4P}$$

$$N = \frac{(R_1 + 1)(L_1 + 1) + (R_2 + 1)(L_2 + 1) + \dots + (R_n + 1)(L_n + 1) - 1}{P + n}$$

In the above equations n is the number of the various types of bones, L and R is the number of left and right elements respectively, subscripts 1, 2, ..., n denote each skeletal element under study (e.g., 1 = femora, 2 = tibiae, etc.), and P is the sum of all pairs.

Example

Consider the following assemblage of human skeletal elements:

Femora: R = 9, L = 9, P = 6

Tibiae: R = 7, L = 7, P = 4

Humeri: R = 7, L = 9, P = 2

Lincoln's Index gives the following estimates:

$N_{\text{femora}} = (9 \times 9) / 6 = 13.5$, thus 14 individuals

$N_{\text{tibiae}} = (7 \times 7) / 4 = 12.25$, thus 12 individuals

$N_{\text{humeri}} = (7 \times 9) / 2 = 31.5$, thus 32 individuals

The discrepancy of the obtained values from different elements is due to the differential preservation of these elements and in our case it is attributed to the small number of pairs identified between right and left humeri. The average MLNI value is 19. In contrast, the values obtained from equations employing multiple elements simultaneously are:

$$N = (9 \times 9 + 7 \times 7 + 7 \times 9) / (6 + 4 + 2) = 193 / 12 = 16.1$$

$$N = (9 + 7 + 7 + 9 + 7 + 9)^2 / (4 \times 3 \times (6 + 4 + 2)) = 2304 / 144 = 16$$

$$N = ((9 + 9)^2 + (7 + 7)^2 + (7 + 9)^2) / ((4 \times (6 + 4 + 2))) = 776 / 48 = 16.2$$

$$N = ((9 + 1)(9 + 1) + (7 + 1)(7 + 1) + (7 + 1)(9 + 1)) / ((6 + 4 + 2) + 3) - 1 = 244 / 15 - 1 = 15.3$$

It is seen that the first three equations employing multiple elements yield the same result, $N = 16$, and this may be adopted as the most likely number of individuals for the assemblage under consideration.

MNI versus MLNI

The MLNI estimates the original number of individuals that comprised the skeletal assemblage, whereas the MNI expresses only a minimum estimate. Furthermore, it is possible to provide confidence intervals with the MLNI, but not with the MNI. Thus, the MLNI should be preferred over the MNI, but in highly fragmented remains, estimation of the MNI may be the only viable option.

SEX ASSESSMENT

In commingled assemblages, sex assessment has to be performed on an element by element basis, except for cases of small-scale commingling where most elements have been sorted per skeleton. The methods that may be adopted are given in STARC Guide no. 1. As most morphological traits for sexing focus on the pelvis and the skull, most disassociated bones will remain unsexed. For this reason, we would recommend the additional adoption of metric methods for sex estimation from the postcranial skeleton, always bearing in mind the population-specificity of these methods and the potential impact of secular change. A compilation of worldwide studies on metric sex estimation using different skeletal elements can be found in Nikita (2017).

AGE-AT-DEATH ESTIMATION

In commingled assemblages, age estimation also has to be performed on an element by element basis, except for cases of small-scale commingling where most elements have been sorted per skeleton. Age-at-death is very difficult to estimate from isolated elements and most elements can only be

assigned to the general "adult" or "nonadult" categories based on their size. All fully fused or 'adult-sized' bone fragments and all permanent teeth with closed root apices and some degree of dental wear will be classified as "adult". Deciduous teeth, still forming permanent teeth, bones with unfused epiphyses (except for late-fusing elements) and all bones that are clearly too small to be adult will be classified as "nonadult". In cases where the skeletal or dental elements preserve sufficient information (e.g. the pubic symphysis or auricular surface on the os coxa), traditional methods for estimating skeletal age-at-death should be used (see STARC Guide no. 1).

The age-at-death distribution of an assemblage comprised of commingled individuals should be established using the most abundant skeletal element that can be sided and aged (Siebke et al. 2019), except in cases of small-scale commingling, where the skeletal elements have been largely sorted per individual skeleton.

PATHOLOGICAL LESIONS

In commingled assemblages the fact that pathological lesions are identified on individual skeletal elements and their overall distribution on the skeleton cannot be examined, limits the potential of accurate diagnosis. In addition, it is difficult to estimate the actual prevalence of a pathological condition in the assemblage. Nonetheless, as highlighted by Brickley and Buckberry (2015), there is still great value in the palaeopathological analysis of partial and poorly preserved skeletons as important information can be obtained for conditions that affect the entire skeleton (e.g. metabolic bone diseases) or conditions which can be diagnosed in individual elements (e.g. osteoarthritis, fractures). See STARC Guide no. 1 for a brief description of different pathological conditions that may be identified on skeletal elements.

ACTIVITY MARKERS

See STARC Guide no. 1 for information on long bone cross-sectional geometric properties, enthesal changes, dental wear and osteoarthritis. When estimating cross-sectional geometric properties on isolated long bones, it may be impossible to standardize biomechanical properties using body mass as a proxy for body size (Ruff 2008). In such cases, powers of bone length may be used: for second moments of area the recommended power is (bone length)^{5.33}, whereas for the total area it is (bone length)³ (Ruff et al. 1993).

NONMETRIC TRAITS

See STARC Guide no. 1 for information on cranial, postcranial and dental nonmetric traits. Note that traits which exhibit a bilateral expression are often inspected on both sides of the body and subsequently the strongest degree of expression is the one recorded in the database. In cases of commingled remains (e.g. loose teeth or unassociated long bones belonging to multiple individuals) it may be impossible to assess which elements form pairs. In such cases, it is advisable to record nonmetric traits only on one side (either the right or the left) in order to avoid having the same individual twice in the dataset, which would bias the results.

MORPHOSCOPIC TRAITS

See STARC Guide no. 1 for information on morphoscopic traits.

METRICS

See STARC Guide no. 1 for cranial, postcranial and dental measurements.

STATURE ESTIMATION

As explained in STARC Guide no. 1, stature estimation from skeletal remains is based on anatomical and mathematical methods. Anatomical methods are not possible to use

with commingled remains except for cases of small-scale commingling, where a full re-association of all elements per skeleton has been accomplished. Regarding mathematical methods, whereas in articulated skeletons it is advisable to use the long bones of the lower limbs when estimating stature by means of regression equations, in disarticulated remains, every available element may/should be used. STARC Guide no. 1 gives representative equations for European and American populations, while Nikita (2017) provides a compilation of population-specific studies which use not only long bones but also other skeletal elements. Finally, as commingled remains are often also fragmented, stature estimation may be based on equations proposed for fragmented remains (e.g. Bidmos 2008). When estimating stature using regression equations, it is imperative to check the standard error of estimate as equations using short bones and fractured elements usually have higher error rates. This fact, coupled with the population-specificity of relevant equations and the effect of secular change, may render stature estimation impractical in many cases.

POST-MORTEM BONE ALTERATION

See STARC Guide no. 1 for post-mortem bone alteration. Note that many different agents can produce the same morphological bone alterations and their discrimination will be especially difficult in commingled remains where assessment often needs to be made on an element-by-element basis.

ADDITIONAL RESOURCES

Online database for recording human commingled remains:

Osterholtz AJ. 2018. *A FileMaker Pro database for use in the recording of Commingled and/or Fragmentary Human Remains*. Mississippi State University: Department of Anthropology and Middle Eastern Cultures. <http://hdl.handle.net/11668/14276>

Documentation for the above database:

Osterholtz AJ. 2019. Advances in documentation of commingled and fragmentary remains. *Advances in Archaeological Practice* 7: 77–86

REFERENCES

- Adams BJ. 2014. *Commingled remains: Field recovery and laboratory analysis*. In: Smith C (ed.) *Encyclopedia of Global Archaeology*. New York: Springer; p. 1575-1580
- Adams BJ, Konigsberg LW. 2004. Estimation of the Most Likely Number of Individuals from commingled human skeletal remains. *American Journal of Physical Anthropology* 125: 138–151
- Adams BJ, Byrd JE. 2006. Resolution of small-scale commingling: A case report from the Vietnam War. *Forensic Science International* 156: 63–69
- Adams BJ, Byrd JE (eds.) 2008. *Recovery, Analysis, and Identification of Commingled Human Remains*. New York: Springer
- Adams BJ, Byrd JE (eds.) 2014. *Commingled Human Remains: Methods in Recovery, Analysis, and Identification*. San Diego: Academic Press
- Anastopoulou I, Karakostis, FA, Borrini M, Moraitis K. 2018. A statistical method for reassociating human tali and calcanei from a commingled context. *Journal of Forensic Sciences* 63: 381-385
- Anastopoulou I, Karakostis, FA, Moraitis K. 2019. A reliable regression-based approach for reassociating human skeletal elements of the lower limbs from commingled assemblages. *Journal of Forensic Sciences* 64: 502-506
- Beckett J, Robb J. 2006. *Neolithic burial taphonomy, ritual and interpretation in Britain and Ireland: A review*. In: Gowland R, Knüsel CJ (eds.) *The Social Archaeology of Funerary Remains*. Oxford: Oxbow Books; p. 57-80
- Bidmos MA. 2008. Stature reconstruction using fragmentary femora in South Africans of European descent. *Journal of Forensic Sciences* 53: 1044-1048
- Brickley MB, Buckberry J. 2015. Picking up the pieces: Utilizing the diagnostic potential of poorly preserved remains. *International Journal of Paleopathology* 8: 51–54
- Budd P, Montgomery J, Barreiro B, Thomas RG. 2000. Differential diagenesis of strontium in archaeological human dental tissues. *Applied Geochemistry* 15: 687-694
- Buikstra JE, Gordon CC, St. Hoyme L. 1984. *The case of the severed skull. Individuation in forensic anthropology*. In: Rathbun TA, Buikstra JE (eds.) *Human Identification: Case Studies in Forensic Anthropology*. Springfield, IL: Charles C. Thomas; p. 121–135
- Byrd JE. 2008. *Models and methods for osteometric sorting*. In: Adams BJ, Byrd JE (eds.) *Recovery, Analysis, and Identification of Commingled Human Remains*. New York: Springer; p. 199-220
- Byrd JE, Adams BJ. 2003. Osteometric sorting of commingled human remains. *Journal of Forensic Sciences* 48: 717-724
- Byrd JE, LeGarde CB. 2014. *Osteometric sorting*. In: Adams BJ, Byrd JE (eds.) *Commingled Human Remains: Methods in Recovery, Analysis, and Identification*. San Diego: Academic Press; p. 167-192

- Calleja M. 2016. *Commingled Tombs and ArcGIS: Analyzing the Mortuary Context and Taphonomy at Bronze Age Tell Abraq*. Masters Dissertation, University of Nevada, Las Vegas
- Castro W, Hoogewerff J, Latkoczy C, Almirall JR. 2010. Application of laser ablation (LA-ICP-SF-MS) for the elemental analysis of bone and teeth samples for discrimination purposes. *Forensic Science International* 195: 17-27
- Chaplin R. 1971. *The Study of Animal Bones from Archaeological Sites*. London: Seminar Press
- Christensen AM, Passalacqua NV, Bartelink EJ. 2014. *Forensic Anthropology: Current Methods and Practice*. San Diego: Academic Press
- Cox M, Flavel A, Hanson I, Laver J, Wessling R. 2008. *The Scientific Investigation of Mass Graves*. Cambridge: Cambridge University Press
- Darrah TH, Prutsman-Pfeiffer JJ, Poreda RJ, Campbell ME, Hauschka PV, Hannigan RE. 2009. Incorporation of excess gadolinium into human bone from medical contrast agents. *Metallomics* 1: 479-488
- Duday H. 1985. *Nouvelles observations sur la décomposition des corps dans un espace libre. Méthode d'étude des sépultures. Saint-Germain en Laye: Nouvelles de l'Archéologie*. Supplément à MSH Informations Paris; p. 6-13
- Duday H. 2005. *L'Archéothanatologie ou l'Archéologie de la Mort*. In: Dutour O, Hublin J-J, Vandermeesch B (eds.) *Objets et Méthodes en Paléanthropologie*. Paris: Comité des Travaux Historiques et Scientifiques; p. 153-215
- Duday H. 2009. *The Archaeology of the Dead: Lectures in Archaeothanatology*. Oxford: Oxbow Books
- Dupras TL, Schultz JJ, Wheeler SM, Williams LJ. 2012. *Forensic Recovery of Human Remains. Archaeological Approaches*, 2nd edition. Boca Raton: CRC Press
- Emberling G, Robb J, Speth J, Wright H. 2002. Kunji cave: early bronze age burials in Luristan. *Iranian Antiquities* 37: 47-104
- Finnegan M. 1988. *Variation of Trace Elements Within and Between Skeletons Using Multiple Sample Sites*. Paper presented at the 15th Annual Meeting of the Paleopathology Association, Kansas City, MO
- Gonzalez-Rodriguez J, Fowler G. 2013. A study on the discrimination of human skeletons using X-ray fluorescence and chemometric tools in chemical anthropology. *Forensic Science International* 231: 407.e1-6
- Grupe G. 1988. Impact of the choice of bone samples on trace element data in excavated human skeletons. *Journal of Archaeological Science* 15: 123-129
- Hines DZC, Vennemeyer M, Amory S, Huel RLM, Hanson I, Katzmarzyk C, Parsons TJ. 2014. *Prioritized sampling of bone and teeth for DNA analysis in commingled cases*. In: Adams BJ, Byrd JE (eds.) *Commingled Human Remains: Methods in Recovery, Analysis, and Identification*. San Diego: Academic Press; p. 275-305
- Holland MM, Cave CA, Holland CA, Bille TW. 2003. Development of a quality, high throughput DNA analysis procedure for skeletal samples to assist with the identification of victims from the world trade center attacks. *Croatian Medical Journal* 44: 264-272
- Just RS, Leney MD, Barritt SM, Los CW, Smith BC, Holland TD, Parsons TJ. 2009. The use of mitochondrial DNA single nucleotide polymorphisms to assist in the resolution of three challenging forensic cases. *Journal of Forensic Sciences* 54: 887-891
- Knüsel CJ, Robb J. 2016. Funerary taphonomy: An overview of goals and methods. *Journal of Archaeological Science: Reports* 10: 655-673
- Konigsberg LW, Adams BJ. 2014. *Estimating the number of individuals represented by commingled human remains: A critical evaluation of methods*. In: Adams BJ, Byrd JE (eds.) *Commingled Human Remains: Methods in Recovery, Analysis, and Identification*. San Diego: Academic Press; p. 193-220
- Lynch JJ, Byrd J, LeGarde CB. 2018. The power of exclusion using automated osteometric sorting: Pair-matching. *Journal of Forensic Sciences* 63: 371-380
- Moutafi I. 2016. *The human remains from Area A*. In: Renfrew AC, Philaniotou O, Brodie N, Gavalas G, Boyd MJ (eds.) *Kavos and the Special Deposits (The sanctuary on Keros and the origins of Aegean ritual practice: the excavations of 2006-2008. Vol. II)*. Cambridge: McDonald Institute for Archaeological Research; p. 483-505
- Mundorff AZ, Shaler R, Bieschke ET, Mar-Cash E. 2014. *Marrying anthropology and DNA: essential for solving complex commingling problems in cases of extreme fragmentation*. In: Adams BJ, Byrd JE (eds.) *Commingled Human Remains: Methods in Recovery, Analysis, and Identification*. San Diego: Academic Press; p. 257-273

REFERENCES

- Naji S, de Becdelièvre C, Djouad S, Duday H, André A, Rottier S. 2014. *Recovery methods for cremated commingled remains: Analysis and interpretation of small fragments using a bioarchaeological approach*. In: Adams BJ, Byrd JE (eds.) *Commingled Human Remains: Methods in Recovery, Analysis, and Identification*. San Diego: Academic Press; p. 33-56
- Nikita E. 2014. Estimation of the original number of individuals using multiple skeletal elements. *International Journal of Osteoarchaeology* 24: 660-664
- Nikita E. 2017. *Osteoarchaeology: A Guide to the Macroscopic Study of Human Skeletal Remains*. San Diego: Academic Press
- Nikita E, Lahr MM. 2011. Simple algorithms for the estimation of the initial number of individuals in commingled skeletal remains. *American Journal of Physical Anthropology* 146: 629-636
- Osterholtz AJ (ed.) 2016. *Theoretical Approaches to Analysis and Interpretation of Commingled Human Remains*. New York: Springer
- Osterholtz AJ, Baustian KM, Martin DL (eds.) 2014a. *Commingled and Disarticulated Human Remains: Working Toward Improved Theory, Method, and Data*. New York: Springer
- Osterholtz AJ, Baustian KM, Martin DL. 2014b. *Introduction*. In: Osterholtz AJ, Baustian KM, Martin DL (eds.) *Commingled and Disarticulated Human Remains: Working Toward Improved Theory, Method, and Data*. New York: Springer; p. 1-13
- Outram AK. 2001. A new approach to identifying bone marrow and grease exploitation: why the “indeterminate” fragments should not be ignored. *Journal of Archaeological Science* 28: 401-410
- Papathanasiou A. 2009. *The human osteological material from the Mycenaean tholos at Kazanaki, Volos*. Proceedings of the 2nd archaeological meeting of Thessaly and Central Greece, Volos, Greece; p. 151-161
- Parsons TJ, Huel R, Davoren J, Katzmarzyk C, Miloš A, Selmanović A, Coble MD, Rizvić A. 2007. Application of novel “mini-amplicon” STR multiplexes to high volume casework on degraded skeletal remains. *Forensic Science International: Genetics* 1: 175-179
- Pemmer B, Roschger A, Wastl A, Hofstaetter JG, Wobraschek P, Simon R, Thaler HW, Roschger P, Klaushofer K, Strelci C. 2013. Spatial distribution of the trace elements zinc, strontium and lead in human bone tissue. *Bone* 57: 184-193
- Perrone A, Finlayson JE, Bartelink EJ, Dalton KD. 2014. *X-ray fluorescence (XRF) for sorting commingled human remains*. In: Adams BJ, Byrd JE (eds.) *Commingled Human Remains: Methods in Recovery, Analysis, and Identification*. San Diego: Academic Press; p. 145-165
- Price TD (ed.) 1989. *The Chemistry of Prehistoric Human Bone*. Cambridge: Cambridge University Press
- Primorac D. 2004. The role of DNA technology in identification of skeletal remains discovered in mass graves. *Forensic Science International* 146: S163–S164
- Puerto MS, Egaña S, Doretti M, Vullo CM. 2014. *A multidisciplinary approach to commingled remains analysis: Anthropology, genetics, and background information*. In: Adams BJ, Byrd JE (eds.) *Commingled Human Remains: Methods in Recovery, Analysis, and Identification*. San Diego: Academic Press; p. 307-335
- Roksandic M. 2002. *Position of skeletal remains as a key to understanding mortuary behavior*. In: Haglund WD, Sorg MH (eds.) *Advances in Forensic Taphonomy: Method, Theory, and Archaeological Perspectives*. Boca Raton: CRC Press; p. 99-117
- Ruff CB. 2008. *Biomechanical analyses of archaeological human skeletons*. In: Katzenberg MA, Saunders SR (eds.) *Biological Anthropology of the Human Skeleton*. New York: Wiley Liss; p. 183-206
- Ruff CB, Trinkaus E, Walker A, Larsen CS. 1993. Postcranial robusticity in Homo. I. Temporal trends and mechanical interpretation. *American Journal of Physical Anthropology* 91: 21-53
- Schaefer M. 2014. *A practical method for detecting commingled remains using epiphyseal union*. In: Adams BJ, Byrd JE (eds.) *Commingled Human Remains: Methods in Recovery, Analysis, and Identification*. San Diego: Academic Press; p. 123-144.
- Seber GAF. 1973. *The Estimation of Animal Abundance and Related Parameters*. London: Griffin
- Shackley SM. 2011. *An introduction to X-ray fluorescence (XRF) analysis in archaeology*. In: Shackley, SM (ed.) *X-Ray Fluorescence Spectrometry (XRF) in Geoarchaeology*. New York: Springer; p. 7-44
- Siebek I, Steuri N, Furtwängler A, Ramstein M, Arenz G, Hafner A, Krause J, Lössch S. 2019. Who lived on the Swiss Plateau around 3300 BCE? Analyses of commingled human skeletal remains from the Dolmen of Oberbipp. *International Journal of Osteoarchaeology* 29: 786-796

- Stevens WD. 2016. *Enslaved Labor in the Gang and Task Systems: A Case Study in Comparative Bioarchaeology of Commingled Remains*. Doctoral dissertation, University of South Carolina
- Thomas RM, Ubelaker DH, Byrd JE. 2013. Tables for the metric evaluation of pair-matching of human skeletal elements. *Journal of Forensic Sciences* 58: 952-956
- Tuller H, Hofmeister U. 2014. *Spatial analysis of mass grave mapping data to assist in the reassociation of disarticulated and commingled human remains*. In: Adams BJ, Byrd JE (eds.) *Commingled Human Remains: Methods in Recovery, Analysis, and Identification*. San Diego: Academic Press; p. 7-32
- Ubelaker DH. 2014. *Commingling analysis: Historical and methodological perspectives*. In: Adams BJ, Byrd JE (eds.) *Commingled Human Remains: Methods in Recovery, Analysis, and Identification*. San Diego: Academic Press; p. 1-6
- Verdugo C, Kassadjikova K, Washburn E, Harkins KM, Fehren-Schmitz L. 2017. Ancient DNA clarifies osteological analyses of commingled remains from Midnight Terror Cave, Belize. *International Journal of Osteoarchaeology* 27: 495-499
- Vickers S, Lubinski PM, DeLeon LH, Bowen JT. 2015. Proposed method for predicting pair matching of skeletal elements allows too many false rejections. *Journal of Forensic Sciences* 60: 102-106
- Westen AA, Gerretsen RRR, Maat GJR. 2008. Femur, rib, and tooth sample collection for DNA analysis in disaster victim identification (DVI). A method to minimize contamination risk. *Forensic Science, Medicine and Pathology* 4: 15–21
- White TE. 1953. A method of calculating the dietary percentage of various food animals utilized by aboriginal peoples. *American Antiquity* 18: 393-399
- Wittmers Jr LE, Wallgren J, Alich A, Aufderheide AC, Rapp Jr G. 1988. Lead in bone. IV. Distribution of lead in the human skeleton. *Archives of Environmental Health: An International Journal* 43: 381-391

RECORDING SHEETS

RECORDING SHEET FOR COMMINGLED HUMAN SKELETAL REMAINS

For cases where the remains have been (partially) sorted by individual, it is advisable to use the form given in STARC Guide no. 1 for articulated skeletons. The forms given here are for individual unassociated skeletal elements. Note that when working with commingled remains, it is generally impractical to use printed forms. Instead, try to fit the information given below in a spreadsheet (e.g. in Excel) whereby each individual element occupies a row and each variable is given in a column.

GENERAL INFORMATION	
Archaeological site:	
Curation site:	
Recorder:	
Date:	
Burial No:	
Grave type:	
Grave size:	
Field methods for site identification:	
Field methods for site excavation:	
Cleaning methods:	
Restoration methods:	

BONE INVENTORY

Key: Zones as defined by Knüsel and Outram (2004); record expression per zone as 0 = absent, 1 = present <25%, 2 = present 26-50%, 3 = present 51-75%, 4 = present >76%, or simply as 0 = absent, 1 = present

CRANIUM, MANDIBLE, EAR OSSICLES & HYOID							
Element	Zone/Side	Expression		Element	Zone/Side	Expression	
Frontal	1			Vomer	-		
	2			Lacrimal			
Parietal	3			Palatine			
	4			Ethmoid	-		
Occipital	5			Mandible	1		
Temporal	6				2		
	7				3		
Sphenoid	8				4		
	9				5		
Zygomatic	10				6		
	11				7		
Maxilla	12			Malleus			
	13			Stapes			
Nasal	14			Incus			
	15			Hyoid	-		
Inferior nasal concha							

THORACIC CAGE & VERTEBRAE							
Element	Zone	Left	Right	Element	Zone	Expression	
Sternum	1			Atlas	1		
	2				2		
	3				3		
					4		
Rib 1	1			Axis	1		
	2				2		
	3				3		
					4		
Rib 2	1			C3-7	1		
	2				2		
	3				3		
					4		
Rib 3-10	1			T1-12	1		
	2				2		
	3				3		
					4		
Rib 11	1			L1-5	1		
	2				2		
	3				3		
					4		
Rib 12	1						
	2						
	3						

SHOULDER GIRDLE			
Element	Zone	Left	Right
Clavicle	1		
	2		
	3		
Scapula	4		
	5		
	6		
	7		
	8		
	9		

UPPER AND LOWER LIMB LONG BONES & PATELLA							
Element	Zone	Left	Right	Element	Zone	Left	Right
Humerus	1			Femur	1		
	2				2		
	3				3		
	4				4		
	5				5		
	6				6		
	7				7		
	8				8		
	9				9		
	10				10		
	11				11		
Radius	1			Patella	-		
	2			Tibia	1		
	3				2		
	4				3		
	5				4		
	6				5		
	7				6		
	8				7		
	9				8		
	10				9		
	11				10		
	J			Fibula	1		
Ulna	A & B				2		
	C				3		
	D				4		
	E				5		
	F				6		
	G						
	H						
	J						

HAND BONES							
Element	Zone	Left	Right	Element	Zone	Left	Right
Scaphoid	-			MC4	1		
Lunate	-				2		
Triquetral	-				3		
Pisiform	-			MC5	1		
Trapezium	-				2		
Trapezoid	-				3		
Capitate	-			Proximal phalanx	1		
Hamate	-				2		
MC1	1				3		
	2			Middle phalanx	1		
	3				2		
MC2	1				3		
	2			Distal phalanx	1		
	3				2		
MC3	1				3		
	2						
	3						

PELVIC BONES							
Element	Zone	Left	Right	Element	Zone	Left	Right
Os coxa	1			Sacrum	1		
	2				2		
	3				3		
	4				4		
	5						
	6						
	7						
	8						
	9						
	10						
	11						
	12						

FOOT BONES							
Element	Zone	Left	Right	Element	Zone	Left	Right
Talus	1			MT3	1		
	2				2		
	3				3		
	4			MT4	1		
Calcaneus	1				2		
	2				3		
	3			MT5	1		
	4				2		
	5				3		
Navicular	-			Proximal phalanx	1		
Cuboid	-				2		
1st Cuneiform	-				3		
2nd Cuneiform	-			Middle phalanx	1		
3rd Cuneiform	-				2		
MT1	1				3		
	2			Distal phalanx	1		
	3				2		
MT2	1				3		
	2						
	3						

UNIDENTIFIED BONE			
Type	Size class	No of fragments	Weight
Cortical	<1 cm		
	1-3 cm		
	3-5 cm		
	>5cm		
Trabecular	<1 cm		
	1-3 cm		
	3-5 cm		
	>5cm		
Cranial	<1 cm		
	1-3 cm		
	3-5 cm		
	>5cm		
Post-cranial	<1 cm		
	1-3 cm		
	3-5 cm		
	>5cm		

DENTAL INVENTORY

Key: 1 = Present, not in occlusion, 2 = Present, development completed, in occlusion, 3 = Missing, no associated alveolar bone, 4 = Missing, antemortem loss, 5 = Missing, postmortem loss, 6 = Missing, congenital absence, 7 = Present, damage renders measurement impossible, 8 = Present, unobservable

PERMANENT TEETH		I1	I2	C	P3	P4	M1	M2	M3
Maxilla	Left								
Maxilla	Right								
Mandible	Left								
Mandible	Right								

DECIDUOUS TEETH		I1	I2	C	M1	M2
Maxilla	Left					
Maxilla	Right					
Mandible	Left					
Mandible	Right					

DENTAL WEAR		I1	I2	C	P3	P4	M1	M2	M3
Maxilla	Left								
	Right								
Mandible	Left								
	Right								

SEX ASSESSMENT (ONLY FOR ADULT REMAINS)

Key: Record as Female, Probable Female, Ambiguous, Probable Male, Male, Indeterminate

Element	Trait/Method	Sex

AGE-AT-DEATH ESTIMATION (FOR NONADULTS)

Classify individuals in one of the following categories: fetus = before birth, infant = 0-3 yrs, child = 3-12 yrs, adolescent = 12-20 yrs, nonadult = <18 yrs, indeterminate = unable to estimate age-at-death

Element	Trait/Method	Sex

AGE-AT-DEATH ESTIMATION (FOR ADULTS)

Classify individuals in one of the following categories: young adult = 20-35 yrs, middle adult = 35-50 yrs, old adult = 50+ yrs, adult = 18+ yrs, indeterminate = unable to estimate age-at-death

Element	Method	Stage	Age

CRANIOMETRICS

Key: All measurements in mm (as defined in Moore-Jansen and Jantz 1989)

Measurement	Type of Value
Maximum cranial breadth	
Minimum frontal breadth	
Upper facial breadth	
Interorbital breadth	
Biorbital breadth	
Bizygomatic diameter	
Nasal breadth	
Nasal height	
Upper facial height	
Orbital height	
Orbital breadth	
Frontal chord	
Basion-bregma height	
Parietal chord	
Maximum cranial length	
Cranial base length	
Basion-prosthion length	
Mastoid length	
Occipital chord	
Maxillo-alveolar length	
Maxillo-alveolar breadth	
Biauricular breadth	
Foramen magnum breadth	
Foramen magnum length	
Chin height	
Bigonial width	
Bicondylar breadth	
Height of the mandibular body	
Breadth of the mandibular body	
Mandibular length	
Maximum ramus height	
Maximum ramus breadth	
Minimum ramus breadth	

POSTCRANIAL MEASUREMENTS

Key: All measurements in mm (as defined in Moore-Jansen and Jantz 1989)

Element	Measurement	Left	Right
Clavicle	Maximum length		
	Superior-inferior (vertical) diameter at midshaft		
	Anterior-posterior (sagittal) diameter at midshaft		
Scapula	Height		
	Breadth		
Humerus	Maximum length		
	Maximum midshaft diameter		
	Minimum midshaft diameter		
	Vertical head diameter		
Ulna	Maximum length		
	Physiological length		
	Minimum circumference		
	Anteroposterior (dorsovolar) diameter		
	Mediolateral (transverse) diameter		
Radius	Maximum length		
	Mediolateral (transverse) midshaft diameter		
	Anteroposterior (sagittal) midshaft diameter		
Os coxa	Height		
	Iliac breadth		
	Ischium length		
	Pubis length		
Sacrum	Anterior length		
	Anterosuperior breadth		
	Maximum transverse base diameter		
Femur	Maximum length		
	Subtrochanteric mediolateral (transverse) diameter		
	Subtrochanteric anteroposterior (sagittal) diameter		
	Midshaft circumference		
	Mediolateral (transverse) midshaft diameter		
	Anteroposterior (sagittal) midshaft diameter		
	Bicondylar length		
	Epicondylar breadth		
	Maximum head diameter		

Element	Measurement	Left	Right
Tibia	Length		
	Circumference at nutrient foramen		
	Mediolateral (transverse) diameter at nutrient foramen		
	Maximum diameter at nutrient foramen		
	Maximum distal epiphyseal breadth		
	Maximum proximal epiphyseal breadth		
Fibula	Maximum length		
	Maximum midshaft diameter		

MEASUREMENTS FOR OSTEOMETRIC SORTING

Key: Record following Byrd and LeGarde (2014)

Element	Measurement	Left	Right
Humerus	Maximum length		
	Epicondylar breadth		
	Capitulum-trochlea breadth		
	Minimum diameter of diaphysis		
Radius	Maximum length		
	Midshaft sagittal diameter		
	Midshaft transverse diameter		
	Maximum shaft diameter at the radial tuberosity		
	Maximum shaft diameter distal to the radial tuberosity		
	Minimum shaft diameter distal to the radial tuberosity		
Ulna	Maximum length		
	Dorso-volar diameter taken perpendicular to the transverse diameter at the same position along the diaphysis		
	Transverse diameter at point of maximum expression of the interosseous crest		
	Minimum diameter of the diaphysis along the portion of the bone that includes the interosseous crest		

Element	Measurement	Left	Right
Femur	Maximum length		
	Epicondylar breadth		
	Maximum head diameter		
	Anterior-posterior subtrochlear diameter		
	Transverse subtrochlear diameter		
Tibia	Maximum length		
	Maximum breadth of proximal epiphysis		
	Maximum breadth of distal epiphysis		
	Maximum diameter at the nutrient foramen		
	Transverse diameter at the nutrient foramen		
	Minimum anterior-posterior diameter of the shaft		
Fibula	Maximum length		
	Maximum midshaft diameter		

MEASUREMENTS FOR OSTEOMETRIC ARTICULATION

Key: Record following Byrd and LeGarde (2014)

Element	Measurement	Left	Right
Scapula	Glenoid fossa max breath		
Humerus	Head A-P breath		
	Capitulum-trochlea breadth		
Radius	Head max diameter		
Ulna	Breadth at distal end of semi-lunar notch		
Os coxa	Max diameter of acetabulum		
Femur	Max head diameter		
	Epicondylar breadth		
Tibia	Max breadth of proximal epiphysis		
	Max breadth of distal epiphysis		
Talus	Min breadth of articular surface		

CRANIAL NONMETRIC TRAITS

Key: Record as present/absent

Trait	Expression	Trait	Expression
Metopic suture		Squamous ossicle	
Supranasal suture		Frontotemporal articulation	
Supraorbital foramina		Marginal tubercle	
Supraorbital notches		Zygomatico-facial foramen	
Ethmoidal foramina		Divided temporal squama	
Infraorbital foramina		Divided zygomatic bone	
Zygomatico-facial foramina		External auditory torus	
Zygomaxillary tubercle		Squamomastoid suture	
Maxillary torus		Parietal foramina	
Transverse palatine suture		Ossicle at lambda	
Palatine torus		Lambdoid ossicles	
Lesser palatine foramina		Ossicle at asterion	
Foramen of Vesalius		Occipitomastoid ossicle	
Oval foramen		Mastoid foramen	
Spinous foramen		Inca bone	
Divided occipital condyles		Coronal ossicle	
Occipitomastoid ossicle		Ossicle at bregma	
Divided parietal bone		Sagittal ossicle	
Parietal notch bone			

MORPHOSCOPIC TRAITS

Key: Record based on Hefner (2009)

Trait	Expression
Inferior nasal aperture	
Anterior nasal spine	
Nasal aperture width	
Nasal overgrowth	
Malar tubercle	
Nasal bone contour	
Interorbital breadth	
Postbregmatic depression	
Supranasal suture	
Transverse palatine suture	
Zygomaxillary suture	

POSTCRANIAL NONMETRIC TRAITS

Key: Record as present/absent

Element	Trait	Expression
Atlas	Double atlas facet	
Cervical vertebrae	Transverse foramen bipartite	
Sternum	Sternal foramen	
Scapula	Bridging of suprascapular notch	
Humerus	Supracondyloid process	
	Septal aperture	
Os coxa	Acetabular crease	
	Accessory sacral facets	
Femur	Allen's fossa	
	Poirier's facet	
	Plaque	
	Hypotrochanteric fossa	
	Third trochanter	
Patella	Vastus notch	
	Emarginate patella	
Tibia	Squatting facets	
Talus	Medial talar facet	
	Lateral talar extension	
	Double inferior anterior talar facet	
Calcaneus	Double anterior calcaneal facet	

DENTAL NONMETRIC TRAITS

Key: Record in an ordinal scale following the ASUDAS system

Tooth	Trait	Expression
Incisors	Winging	
	Shovel-shaped	
	Double shoveling	
	Labial curvature	
	Interruption groove	
	Tuberculum dentale	
	Peg-shaped incisors	
Canines	Distal accessory ridge	
	Lower canine root number	
	Bushman canine	
Premolars	Odontome	
	Upper premolar root number	
	Distosagittal ridge	
	Tome's root	
	Lower premolar lingual cusp variation	
Molars	Carabelli's trait	
	Upper molar root number	
	Enamel extensions	
	Hypocone	
	Metaconule	
	Deflecting wrinkle	
	Anterior fovea	
	Tuberculum intermedium	
	Tuberculum sextum	
Lower molar root number		
Hypoconulid		
Groove pattern		

POST-MORTEM BONE ALTERATION

Key: Record based on Fernández-Jalvo and Andrews (2016)

Alteration	Type	Element(s) affected	Possible etiology

ISBN 978-9963-2858-5-3

PROMISE 



RESEARCH
& INNOVATION
FOUNDATION



Structural Funds
of the European Union in Cyprus